Newly revealed features of fracture toughness behavior of spot welded dual phase steel sheets for automotive bodies

Ibrahim Sevim,
Yenişehir-Mersin, Turkey

Materials Testing downloaded from www.hanser-elibrary.com by Carl Hanser Verlag on November 24, 2015
For personal use only.

Article Information

Correspondence Address
Associate Prof. Dr. İbrahim Sevim
Department of Mechanical Engineering
Faculty of Engineering
Mersin University
33343 Yenişehir-Mersin, Turkey
E-mail: ibrahimsevim33@gmail.com

Keywords
Dual phase steel, automotive body, DP 450 steels, resistance spot welding, fracture toughness, nucleus size ratios h_n/d_n

Fracture toughness is one of the parameters, which are used to estimate the fatigue life of resistance spot-welded (RSW) joints. A spot-welded pair is affected by the shear stress of the weld zone when it is exposed to tensile load. Repetitive loads reduce the fatigue life of the spot weld, and the material splits at the spot-welded region. This study investigates the effect of welding current, weld time and nucleus size ratios on the fracture toughness of RSW of galvanized DP450 steels having 1.0 mm thickness. The specimens were joined by spot welding at different welding currents and times. Welding processes were carried out using 3, 5, 7 and 9 kA welding current and 10, 20, 30 and 40 cycles (1 cycle = 0.02 s) weld time and the electrode pressure was fixed at 600 MPa. All series of specimens were exposed to tensile shear test in order to determine the fracture toughness. The fracture toughnesses for all series of RSW joints were calculated by using the formula given in the literature. The nugget diameters, core sizes and their heights were measured via an optical microscope. The Vickers microhardness measurement was carried out on the weld nugget, heat affected zone (HAZ) and base metal. Nucleus size ratios were calculated. The results of the study demonstrated that the fracture toughness of RSW depended not only on the nugget diameter D, but also sheet thickness t, tensile rupture force F, hardness H and nucleus size ratios h_n/d_n.

High strength steels are commonly used for production of vehicle bodies in the automotive industry in order to reduce weight of the vehicle due to their properties such as good corrosion resistance, high strength and the capability to absorb impacts during any collision. Dual phase (DP) steels are an improved type of high strength low alloy (HSLA) steels. In terms of microstructure, they contain martensite phases in the ferrite matrix. DP steels are manufactured by slowly annealing hypo-eutectoid steels in the critical zone ($\alpha+\gamma$ zone) between A_1-A_3 temperatures in the Fe-C balance diagram and then cooling in a suitable speed to provide martensitic transformation [1-4]. When compared to carbon steels, DP steels are easier to form, they have a low yield stress, a more uniform structure and more elongation [1]. Due to these factors, DP steels have a better plastic forming feature. Since DP steels which have low yield/tensile strength and good forming capability possess a high "strength/weight" relationship, they are suitable for vehicle bodies in order to reduce the vehicle weight and the fuel consumption [5].

DP steels can be joined by using various welding methods. Spot welding is the simplest, cheapest and best welding method for DP steels. Thus, the spot welding is one of the main joining methods in the vehicle body assembly due to its high efficiency in welding thin DP steels. Via the spot welding, DP steel sheets can be welded up to 3-mm thickness [6-7]. The automotive industry uses approximately 3000-5000 spot welds in one vehicle body [8].

The spot welded joints in a vehicle structure are exposed to stresses under both static and dynamic loads during operation. The stress under static loads can be explained by tensile strength tests. However, the type of damage that occurs in the zones constrained under dynamic loads is called fatigue damage which is more critical. The fatigue damage starts due to some fault in the material or discontinuity, progresses and consequently results in fatigue damage. Especially after spot welding, mechanical and metallurgical transformations oc-

Materials Testing downloaded from www.hanser-elibrary.com by Carl Hanser Verlag on November 24, 2015
For personal use only.

cur in the weld zone and in the heat affected zone due to rapid heating and cooling of the weld zone. These transformations considerably affect the strength of the spot weld, especially under dynamic stresses. Thus, welding zones are critical areas which are under stress intensity in terms of the fatigue damage [9-10].

Variables such as shear stress affecting the welding zone, thickness of sheet metal, number of spot welds and the width of the welding zone are important parameters influencing the welded joint in the spot welding. To express the fatigue life of spot welds, expressions of the stress intensity factor are utilized. With the help of these stress intensity factor expressions, the fatigue life of spot welds is estimated. To determine the fracture parameters such as notch stress and stress intensity factor in spot welded joints, approaches of fracture mechanics were used. Approach of fracture mechanics is commonly used in calculating the stress intensity factors for spot welded joints under shear stress [11-12].

The parameter related to fracture in the analysis of fracture mechanics is either the fracture toughness or the stress intensity factor. The stress intensity factor is a parameter that specifies the stress zone near the crack and depends on the geometric situation of the material, the shape of the stress applied and the location of the crack. The essential objective of fracture mechanics is to determine the stress intensity factors. The fracture of a material can occur in three different modes as seen in Figure 1 [11-12]. These are K_I: opening mode, K_{II}: shearing mode and K_{III}: tearing mode, as presented in Figure 1.

There is a limited number of studies conducted on estimating the stress intensity factors of spot welded joints. The first study was conducted by Pook [13]. Pook expressed the stress intensity factor as an equation for spot welds by improving the equations used by Paris Sih and Kassir for elliptic connections [14-15]. Radaj [16] showed that the fatigue strength of spot welded overlaps joints can be calculated by considering the local stress. Zhang [17-18] expressed the relation between stress intensity factor in spot welded overlap joints and J integral. Zhang [17] suggested the below equation for stress intensity factor K_{II} in spot welded overlap joints:

$$K_{II} = \frac{2 \cdot F}{\pi \cdot D\sqrt{S}} (MPa \cdot m^{1/2}) \quad (1)$$

with D: diameter of the spot weld (mm), S: thickness of the sheet metal (mm) and F: shear force (N).

There are studies explaining mechanical properties of spot welded joints in the literature. Wilson and Fine [19] defined the stress intensity. Pan and Sheppard [20] tried to explain the formation of microcracks in the weld zone and to estimate the stress intensity factors for these microcracks. Darwish et al. [21] researched the damage formation rate in spot welded joints based on welding parameters. Chang et al. [22] studied hardness distribution at the interface of welded plaque in spot welded overlap joints.

Chandel and Garber [23] formulated the strength of different spot welded structures (martensitic, bainitic, cold rolled) according to various welding currents and weld times. Zuniga and Sheppard [24] showed how the tensile strength and yield strength of the material change with the hardness of the heat affected zone for galvanized high strength low alloy steel (HSLA).

Tao et al. [25] studied the fracture characteristics of a spot welded DP 600. Marya and Gayden [26] researched fracture of the weld by associating welding parameters and sheet steel characteristics. Baltazar Hernandez et al. [27] investigated on the effects of microstructure and weld sizes on the mechanical behavior of various spot welded AHSS steels.

Hayat and Sevim [28] studied fracture toughness of galvanized DP600 steel sheets welded by RSW depending on welding current and weld time. Sevim et al. [29] worked on the nucleus geometry and mechanical properties of the resistance spot welded coated-uncoated DP automotive steels. However, there is a limited number of studies conducted on investigating the fracture of spot welded joints. Also, there has been no extensive study conducted on examining the fracture toughness of galvanized DP 450 spot welded overlap joints.

This study investigates the effect of welding current, weld time and nucleus size ratios on the fracture toughness of welding joints in the spot welding of DP450 galvanized steels with a thickness of 1.0 mm. The specimens were joined via spot welding at different welding currents and times. Welding processes were done by using 3, 5, 7 and 9 kA welding current and 10-20-30-40 cycle (1 cycle = 0.02 s) welding time and the electrode pressure was fixed at 600 MPa. All series of specimens were exposed to tensile shear test in order to determine the fracture toughness. The fracture toughness of all series of resistance spot welded joints was calculated by using the formula given in the literature. The nugget diameters, core sizes and their heights were measured by means of an optical microscope. The Vickers microhardness measurement across the weld nugget, HAZ and base metal was carried out. Nucleus size ratios were calculated.

Experimental procedure

Material. Galvanized DP450 commercial steel sheets with a thickness of 1.0 mm were used in the experiments. The zinc coating thickness of the DP 450 steels used in the experiments were 23 µm. Table 1 illustrates the chemical composition of the galvanized DP450 commercial steel sheets

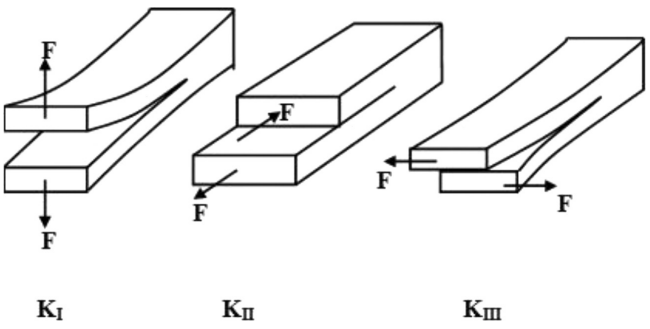

Figure 1: Basic fracture modes K_I: opening mode K_{II}: shearing mode and K_{III}: tearing mode

Material	C	Si	Mn	Cr	Ni	Nb	Ti	V	Mo	Fe
DP450	0.054	0.129	1.32	0.51	0.02	0.0043	0.001	0.004	0.0029	Bal.

Table 1: Chemical composition of the material used in the experiments (wt.-%)

Materials Testing downloaded from www.hanser-elibrary.com by Carl Hanser Verlag on November 24, 2015
For personal use only.

Welding current (kA)	Welding time (cycles)			
	10	20	30	40
3	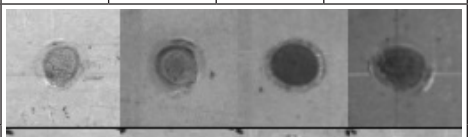			
5	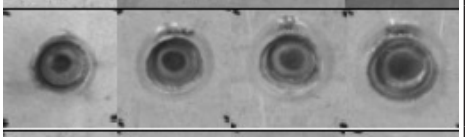			
7	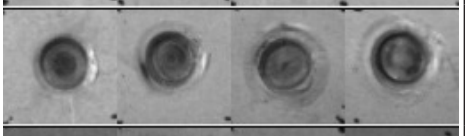			
9	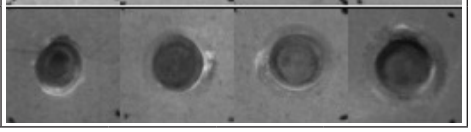			

Table 2: DP450 nugget photographs of spot welded specimen [29]a

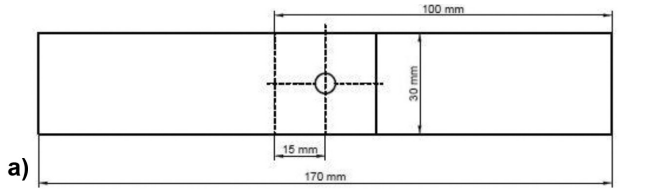

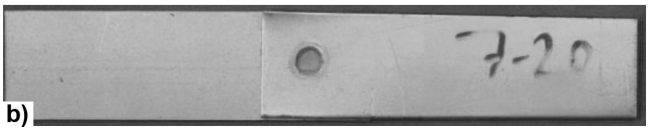

Figure 2: Dimensions of welded samples, a) according to DN17440, b) photo of welded specimen

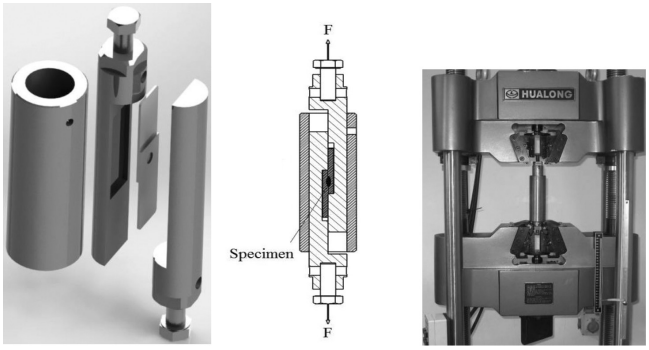

Figure 3: a) Shear mode K_{II} apparatus, b) cut view of apparatus, c) tensile test machine

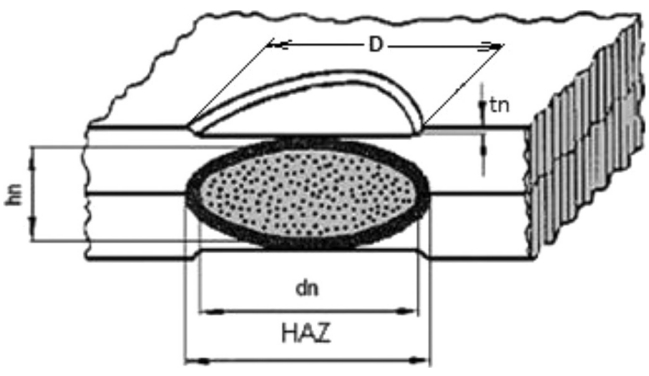

Figure 4: Weld nugget geometry (d_n: nucleus diameter, t_n: deformation depth, h_n: height of nucleus) [30]

that were used in the experiments. For the welding process, galvanized DP450 steel sheet specimens in dimensions of 100 mm x 30 mm were prepared.

Welding process. DP 450 specimens were prepared according to DIN 17440 standard and overlap spot welds were made (see Figures 2a and 2b). Weldings were performed by using the spot weld machine at 60 kVA. Before performing the welding process, the surfaces of the specimens were immersed in alcohol for cleaning and then the spot welds were performed. Cu-Cr alloyed water cooled conical electrodes were used as welding electrode. The contact diameter of the electrodes used in welding process was 8 mm. The geometry of nugget changes with welding current and welding time as seen in Table 2. Resistance spot welds were performed at extrusion pressure of 600 MPa, at welding currents of 3-5-7-9 kA and welding times of 10-20-30-40 cycles (1 cycle = 0.02 s), respectively.

Determination of fracture toughness of RSW. Fracture toughness of RSW galvanized DP 450 steel sheets were calculated according to the tensile shear test results. The welded specimens were fixed to an apparatus as shown in Figure 3 and subjected to tensile shear tests.

After the tensile shear test, three measurements were carried out on the fracture surfaces, as given in Figure 4, regarding weld nugget diameter D, nucleus diameters d_n, deformation depth t_n and heights of the nucleus d_n. The average of these three measurements was recorded. Equation (1) was used to calculate the fracture toughness values. HAZ of spot welding was sanded with 80-1200 mesh sandpaper and was polished with 0.3 µm diamond paste. After the polishing process, the microhardness scanning of the surface was made under 1.96 N (HV 0.2) load.

Results

Variation in fracture toughness K_{IIC} related to nucleus size ratio h_n/d_n. Figure 5 illustrates variation graph of nucleus diameter d_n related to welding current I. Welding time is the variable parameter in the variation of nucleus diameter d_n related to welding current I. Table 3 illustrates the variation equations of nucleus diameter d_n and welding current I, which are dependent on this variable parameter, and the general equation is given in Equation (2).

$$d_n = A \times I^{(1/4)} \quad (2)$$

With d_n: nucleus diameter, A: constant and I: welding current.

Also, as seen in Figure 6, Equation (3) describes the dependance of constant A on welding time.

$$A = B \times t^{(1/5)} \quad (3)$$

With B: constant with its value = 1.0 and t: welding time (s).

Substitution of Equation (3) into Equation (2) reveals:

$$d_n = B \times t^{(1/5)} \times I^{(1/4)} \quad (4)$$

with d_n: nucleus diameter (mm), B: constant, t: welding time and I: welding current.

Figure 7 illustrates a variation graph of the height of the nucleus h_n in terms of welding current I. Welding time is the variable parameter in this graph. Table 4 shows the equations of the height of nucleus h_n related to welding current I, which are dependent on this variable parameter, which can also be expressed by the general Equation (5):

$$h_n = C \times I^{(1/4)} \quad (5)$$

with h_n: height of the nucleus (mm), C: constant and I: welding current.

Also, as seen in Figure 6, Equation (6) describes the dependance of constant C on welding time (see Figure 8):

$$C = E \times t^{(1/5)} \quad (6)$$

with E: constant with its value = 13.2 and t: welding time (s).

Materials Testing downloaded from www.hanser-elibrary.com by Carl Hanser Verlag on November 24, 2015
For personal use only.

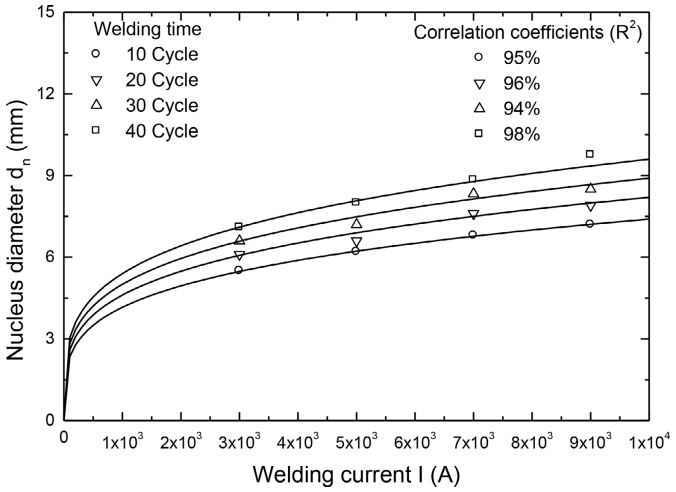

Figure 5: Variation of nucleus diameter d_n related to welding current I (A)

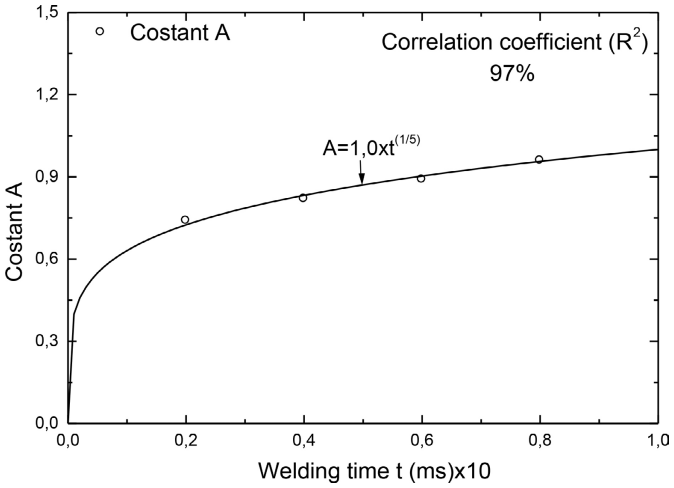

Figure 6: Variation of constant A with weld time

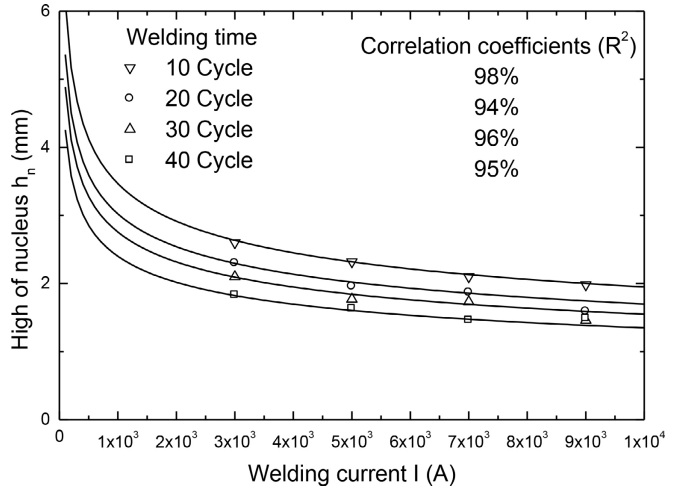

Figure 7: Variation of height of nucleus h_n related to the welding current I (A)

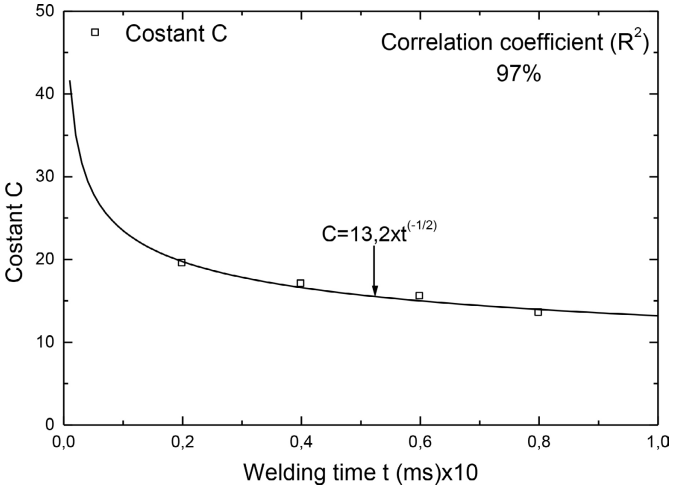

Figure 8: Variation of constant C with weld time

Welding time t (ms) × 10	Equations for KIIC	Constant A
0.2	$d_n = 74 \times 10^{-2} I^{(1/4)}$	74×10^{-2}
0.4	$d_n = 82 \times 10^{-2} I^{(1/4)}$	82×10^{-2}
0.6	$d_n = 89 \times 10^{-2} I^{(1/4)}$	89×10^{-2}
0.8	$d_n = 96 \times 10^{-2} I^{(1/4)}$	96×10^{-2}

Table 3: Constant A in the variation of welding current I with nucleus diameter d_n

Welding time t (ms) × 10	Equations for height of nucleus hn	Constant C
0.2	$h_n = 19.5 I^{(1/4)}$	19.5
0.4	$h_n = 17 I^{(1/4)}$	17.0
0.6	$h_n = 15.5 I^{(1/4)}$	15.5
0.8	$h_n = 13.5 I^{(1/4)}$	13.5

Table 4: Constant C in the variation of height of nucleus h_n with welding current I

$$h_n = \frac{E \cdot t^{(1/5)}}{I^{(1/4)}} \quad (7)$$

With d_n: nucleus diameter (mm), E: constant, t: welding time and I: welding current.

Figure 9 illustrates a variation graph of the nucleus size ratio h_n/d_n related to welding current. Welding time is the variable parameter in this graph. Table 5 shows the equations of nucleus size ratio h_n/d_n related to welding current, which are dependent on this variable parameter, which can be also expressed by the general Equation (8):

$$\frac{h_n}{d_n} = \frac{J}{I^{1/2}} \quad (8)$$

with h_n/d_n: nucleus size ratio, J: constant and I: welding current.

Also, as seen in Figure 10, Equation (9) describes the dependance of constant J on welding time:

$$J = K \times t^{(-1/2)} \quad (9)$$

with K: constant with its value 13 and t: welding time (ms).

$$\frac{h_n}{d_n} = \frac{K}{\left(I \cdot t\right)^{1/2}} \quad (10)$$

With K: dimensional constant.

Figure 11 illustrates a variation graph of fracture toughness K_{IIC} related to nucleus size ratio h_n/d_n. Welding time is the variable parameter in this graph. Table 6 illustrates the equations of fracture toughness K_{IIC} related to nucleus size ratio h_n/d_n, which are dependent on this variable parameter, which can also be expressed by the general Equation (11):

$$K_{IIC} = \frac{h_n}{d_n}\left(L - M \cdot \frac{h_n}{d_n}\right) \quad (11)$$

with K_{IIC}: fracture toughness, L and M: constants and $\frac{h_n}{d_n}$: nucleus size ratio.

Also, as seen in Figure 12, Equation (12) below can be obtained from the variation graph of constant K related to welding time:

$$L = N \times t^{(1/4)} \quad (12)$$

with N: constant with its value 340 and t: welding time (ms).

Also, as seen in Figure 13, Equation (13) below describes the dependance of constant M on welding time:

$$M = P \times t^{(3/4)} \quad (13)$$

with P: constant with its value 1200 and t: welding time (ms).

Substitution of the Equations (12) and (13) into Equation (11) reveals:

$$K_{IIC} = \frac{h_n}{d_n} \cdot t^{(1/2)} \cdot \left(N - P \cdot t \cdot \frac{h_n}{d_n}\right) \quad (14)$$

with N and P: dimensional constants.

The variation of fracture toughness related to welding current and hardness.

Figure 14 illustrates the variation of fracture toughness K_{IIC} related to Vickers hardness. Welding current is the variable parameter in this graph. Table 7 illustrates the equations of variation of fracture toughness K_{IIC} related to Vickers hardness, which are dependent on this variable parameter, which can also be expressed by the general Equation (15):

$$K_{IIC} = H(T - U \times H) \quad (15)$$

with K_{IIC}: fracture toughness, T and U: constants and H: average Vickers hardness of the weld nugget.

According to Figure 15, the constant T can be expressed as a function of welding current:

$$T = \frac{I^{(1/5)}}{85 \cdot 10^4} \quad (16)$$

with V: constant dependent on t: welding time (ms) and I: welding current.

When this Equation (16) is inserted into Equation (15), Equation (17) is obtained:

$$K_{IIC} = H\left(\frac{I^{(1/5)}}{V} - \frac{33}{10^6} \cdot H\right) \quad (17)$$

Welding time t (ms) × 10	Equations for nucleus size ratio (h_n/d_n)	Constant J
0.2	$\frac{h_n}{d_n} = 26I^{(-1/2)}$	26
0.4	$\frac{h_n}{d_n} = 20.5I^{(-1/2)}$	20.5
0.6	$\frac{h_n}{d_n} = 17.5I^{(-1/2)}$	17.5
0.8	$\frac{h_n}{d_n} = 14.5I^{(-1/2)}$	14.5

Table 5: Constant J in the variation of nucleus size ratio h_n/d_n with welding current

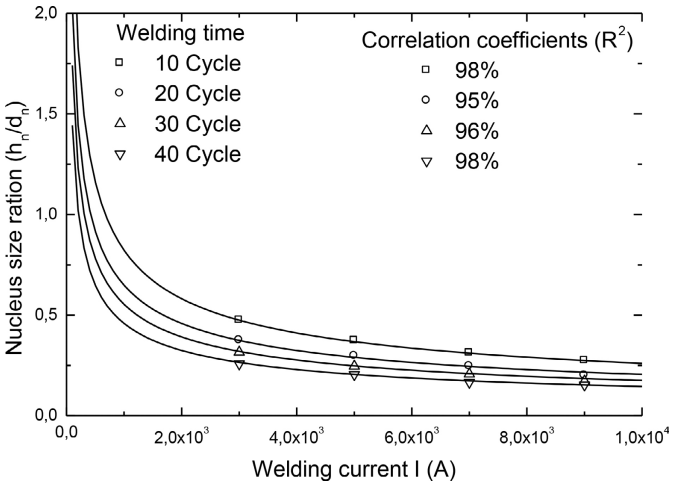

Figure 9: Variation of nucleus size ratio h_n/d_n related to the welding current I (A)

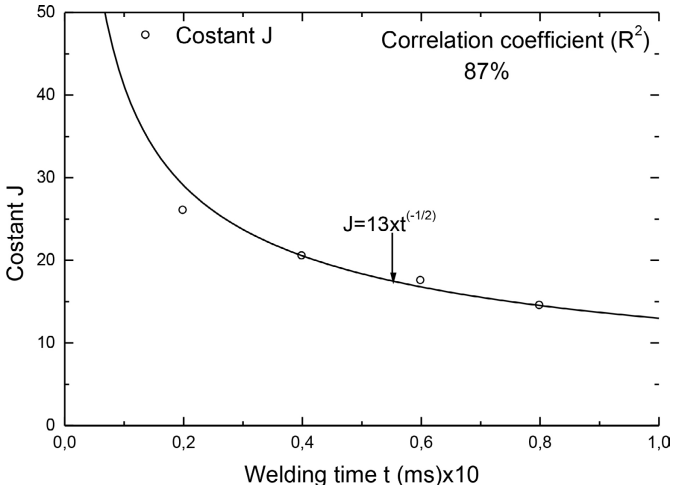

Figure 10: Variation of constant J related to weld time

Materials Testing downloaded from www.hanser-elibrary.com by Carl Hanser Verlag on November 24, 2015
For personal use only.

As seen in Equation (17), the fracture toughness K_{IIC} depends on both the welding current and the hardness of the weld zone.

Discussion

The variables that affect the microstructure of the weld zone are welding current I, welding time t, chemical composition of galvanized DP 450 steel and the cooling rate of the weld zone. The formation of various microstructures depends on these variables. As these parameters change, the microstructure changes as well.

The heat input during the RSW can be calculated from the Equation (18) [30-31]:

$$Q = I^2 \times R \times t \quad (18)$$

with Q: total generated heat (J), I: welding current (A), R: total resistance of the welded part (Ω) and t: welding time (ms).

As seen in Equation (18), total generated heat is proportional to the square of welding current and welding time. Welding current and welding time affect the amount of the metal melted during the welding process. This also affects the weld nugget diameter and the microstructure of the weld zone due to the melting phenomena. As seen in the Equations (9), (13) and (15) for spot welded overlap joints with galvanized DP 450 sheets, the welding current I, welding time t, nucleus size ratio h_n/d_n and the hardness of the weld zone also affect the fracture toughness.

The nugget weld zone has similar properties to cast metal structures. The hardness of the zone is greater than of the base

Welding time t (ms) × 10	Equations for KIIC	Constant L	Constant M
0.2	$K_{IIC} = 218\left(\frac{h_n}{d_n}\right) - 375\left(\frac{h_n}{d_n}\right)^2$	218	375
0.4	$K_{IIC} = 265\left(\frac{h_n}{d_n}\right) - 575\left(\frac{h_n}{d_n}\right)^2$	265	575
0.6	$K_{IIC} = 285\left(\frac{h_n}{d_n}\right) - 720\left(\frac{h_n}{d_n}\right)^2$	285	720
0.8	$K_{IIC} = 345\left(\frac{h_n}{d_n}\right) - 1100\left(\frac{h_n}{d_n}\right)^2$	345	1100

Table 6: Constants L and M in the variation of fracture toughness with nucleus size ratio h_n/d_n

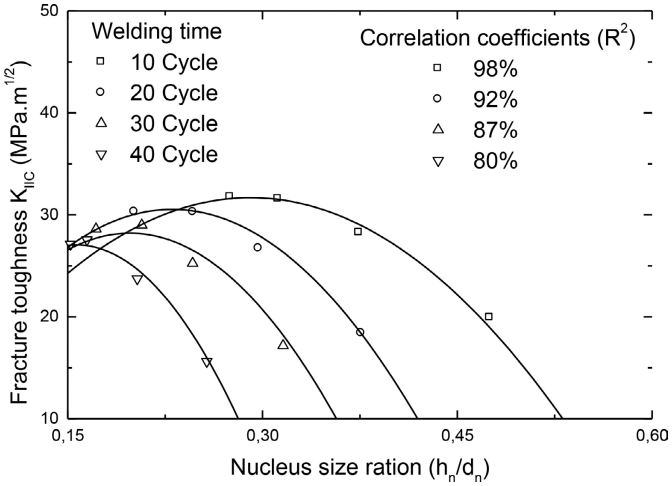

Figure 11: Variation of fracture toughness K_{IIC} related to nucleus size ratio h_n/d_n

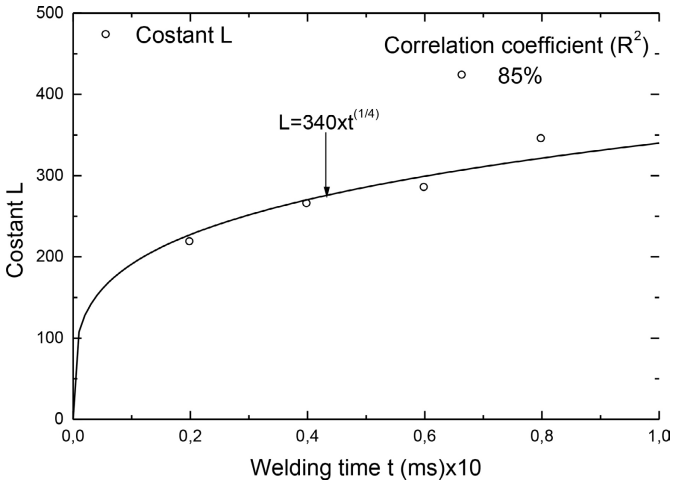

Figure 12: Variation of constant L related to weld time

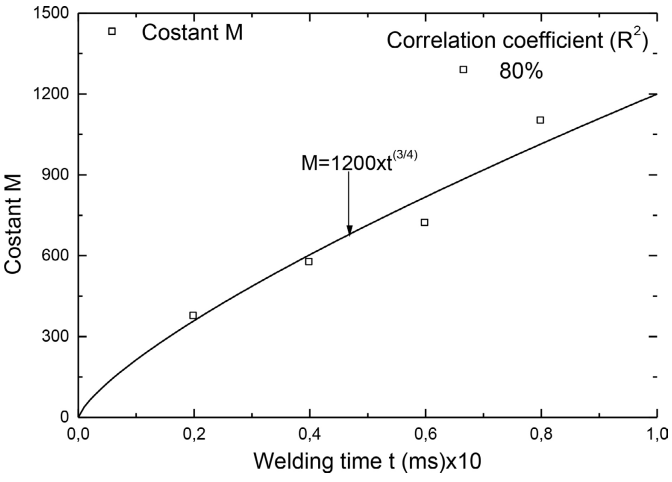

Figure 13: Variation of constant M related to weld time

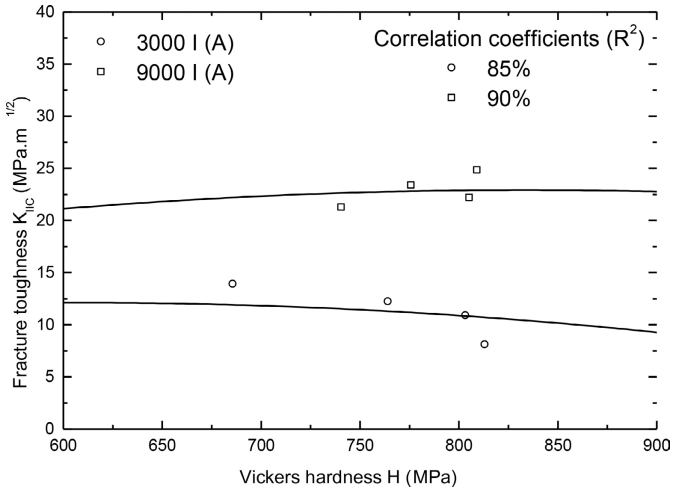

Figure 14: Fracture toughness K_{IIC} versus Vickers hardness H

Materials Testing downloaded from www.hanser-elibrary.com by Carl Hanser Verlag on November 24, 2015
For personal use only.

Welding current I (kA)	Equations for KIIC	Constant T	Constant U
3	$K_{IIC} = 55 \times 10^{-3}H - 33 \times 10^{-6}H^2$	55×10^{-3}	33×10^{-6}
9	$K_{IIC} = 4 \times 10^{-2}H - 33 \times 10^{-6}H^2$	4×10^{-2}	33×10^{-6}

Table 7: Constants T and U in the variation of fracture toughness with hardness H

metal. The hardness of the martensitic structure forming in the weld zone related to the carbon content can be expressed as follows [32]:

$$H_M = 884 \times C(1 - 0.03 \times C^2) + 294 \qquad (19)$$

with H_M: hardness of martensitic structure and C: carbon rate of the alloy.

The hardness of the nugget of the weld zone of the specimen, which is calculated using Equation (19), is $H_M = 669$ (MPa). This is the smallest hardness value required for the formation of the martensitic structure. It could be concluded from this data that the nugget of the weld for the specimen completely transformed to the martensite structure. Since the weld zone is a melted area, it acts similar to the cast metal structures in other words they are hard and brittle. Related to the cooling rate of the weld zone, shrinkage and cold cracks occur easily [2]. Due to the fact that coherent granules and particle borders are probably crack starting points, these also help the cracks to proceed and cause damage at the end of resistance spot welded joints [11-12].

Conclusions

This study is focused on fracture toughness of RSW DP 450 sheets used in automotive body. Following conclusions can be drawn according to the above results:

- When welding time and/or welding current increase, nugget diameter and weld penetration depth increase. These parameters affect fracture toughness.
- When the welding time is short and the welding current is low, nugget diameter and fracture toughness decrease.
- Nucleus size ratio h_n/d_n is inversely proportional.
- Lower welding time and welding current increase nucleus size ratio h_n/d_n.
- Fracture toughness of RSW joints is proportional to welding current and welding time.
- Fracture toughness in resistance spot welds does not only depend on the nucleus diameter D, but it also depends on sheet metal thickness S, shear tensile load F, welding current I, welding time t and nucleus size ratio h_n/d_n.
- Nucleus size diameter d_n is depended on welding current and welding time as described by Equation (4).
- Height of the nucleus h_n can be determined by Equation (7) using welding current and welding time.
- Nucleus size ratio h_n/d_n can be assessed from Equation (10) using welding current and welding time.
- Fracture toughness of RSW joints can be calculated from Equation (14).

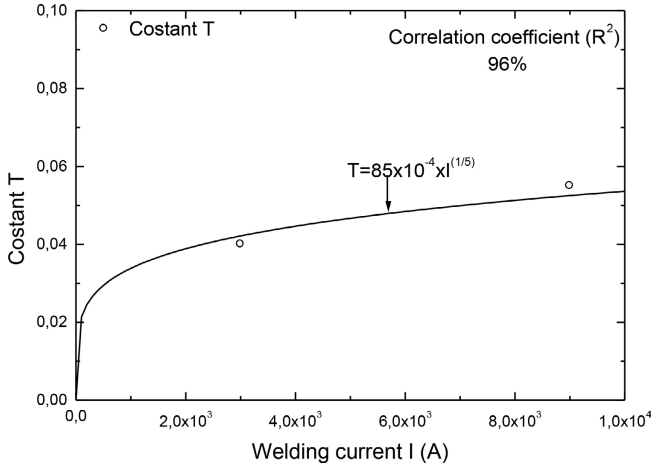

Figure 15: Constant T dependent on welding current I (A)

References

1 F. Ozturk, S. Toros, S. Kilic: Tensile and springback behavior of DP600 advanced high strength steel at warm temperatures, J. Iron Steel Res. Int. 16 (2009), pp. 41-46 DOI:10.1016/S1006-706X(10)60025-8

2 C. Ma, D. L. Chen, S. D. Bhole, G. Boudreau, A. Lee, E. Biro: Microstructure and fracture characteristics of spot-welded DP600 steel, Mater. Sci. Eng. A 485 (2008), pp. 334-346 DOI:10.1016/j.msea.2007.08.010

3 L. Xinsheng, W. Xiaodong, G. Zhenghongz, W. Min, W. Yixiong, R Younghua: Microstructures in a resistance spot welded high strength dual phase steel, Mater. Char. 61 (2010), pp. 341-346 DOI:10.1016/j.matchar.2009.12.018

4 M. Kleiner, S. Chatti, A. Klaus: Metal forming techniques for lightweight construction, J. Mater. Proc. Technol. 177 (2006), pp. 2-7 DOI:10.1016/j.jmatprotec.2006.04.085

5 X. Q. Zhang, G. L. Chen, Y. S. Zhang: Characteristics of electrode wear in resistance spot welding dual-phase steels, Mater. Des. 29 (2008), pp. 279-283 DOI:10.1016/j.matdes.2006.10.025

6 F. Hayat, B. Demir, S. Aslanlar, M. Acarer: Effect of welding time and current on the mehanical properties of resistance spot welded IF (DIN EN 10130-11999) steel, Kov. Mat. 47 (2009), pp.11-17

7 F. Hayat, B. Demir, M. Acarer: Tensile shear stress and microstructure of low-carbon dual phase Mn-Ni steels after spot resistance welding, M. Sci. Heat Treat. 49 (2007), pp. 484-489 DOI:10.1007/s11041-007-0090-x

8 A. Bak, S. Gunduz: Effect of strain ageing on the mechanical properties of interstitial free steels under as-received, heat treated and spot welded conditions for automotive applications, Proc. of the Institution of Mechanical Engineers Part D-J. Automob. Eng. 209 (2009), pp. 785-791 DOI:10.1243/09544070JAUTO1176

9 M. Erdogan: The effect of new ferrite content on tensile fracture behaviour of dual-phase steels, J. Mat. Sci. 37 (2002), pp. 3623-3630 DOI:10.1023/A:1016548922555

10 M. K. Kulekci, F. Mendi, I. Sevim, O. Basturk: Fracture toughness of friction stir welded joints of AlCu4SiMg aluminium alloy, Metalurgija 44 (2005), pp. 209-213

11 I. Sevim: Fracture toughness of spot-welded steel joints, Kov. Mat. 43 (2005), pp. 113-123

12 I. Sevim: Effect of hardness on fracture toughness for spot-welded steel sheets, Mater. Des. 27 (2006), pp. 21-30 DOI:10.1016/j.matdes.2004.09.008

13 L. P. Pook: Fracture mechanics analysis of the fatigue behavior of spot welds, Int. J. Fract. 11 (1975), pp. 173-176 DOI:10.1007/BF00034726

14 P. C. Paris, G. C. Sih: Fracture toughness testing and its application, ASTM STP 381 (1965), p. 30

15 G. C. Sih: Handbook of Stress Intensity Factors, Lehigh University, Bethlehem, Pennsylvania, USA (1973)

16 D. Radaj, S. Zhang: Stress intensity factors for spot welds between plates of dissimilar materi-

Materials Testing downloaded from www.hanser-elibrary.com by Carl Hanser Verlag on November 24, 2015
For personal use only.

als, Engineering Fracture Mechanics 42 (1992), pp. 407-426
DOI:10.1016/0013-7944(92)90163-9
17 D. Zhang: Stress intensities at spot welds, Int. J. Fract. 88 (1997), pp. 167-185
DOI:10.1023/A:1007461430066
18 D. Zhang: Stress intensities derived from stresses around a spot weld, Int. J. Fract. 99 (1999), pp. 239-257
DOI:10.1023/A:1018608615567
19 B. Wilson, T. E. Fine: Fatigue behavior of spot-welded high strength steel joints, SAE Technical Paper No. 810354 (1981)
DOI:10.4271/810354
20 N. Pan, S. D. Sheppard: Stress intensity factors in spot welds, Eng. Fract. Mech. 70 (2003), pp. 671-684
DOI:10.1016/S0013-7944(02)00076-0
21 S. M. Darwish, M. S. Soliman, A. M. Al-Fahead: Manufacturing and characteristics of brass damping sheets, J. Mater. Process. Technol. 79 (1998), pp. 66-71
DOI:10.1016/S0924-0136(97)00322-1
22 B. Chang, S. Y. Yaowu, L. Lu: Studies on the stress distribution and fatigue behavior of weld-bonded lap shear joints, J. Mater. Process. Technol. 108 (2001), pp. 307-313
DOI:10.1016/S0924-0136(00)00842-6
23 R. S. Chandel, S. Garber: Mechanical and metallurgical aspects of spot-welded joints, Met. Technol. 1 (1974), pp. 418-424
DOI:10.1179/030716974803287645
24 S. M. Zuniga, S. D. Sheppard: Determining the constitutive properties of the heat-affected zone in a resistance spot weld, Modeling Simul. Mater. Sci. Eng. A. 3 (1995), pp. 391-416
DOI:10.1088/0965-0393/3/3/007
25 H. Tao, P. D. Zavattieri, L. G. Jr. Hector, W. Tong: Mode I fracture at spot welds in dual-phase steel: An application of reverse digital image correlation, Experimental Mechanics 50 (2010), pp. 1199-1212
DOI:10.1007/s11340-009-9323-9
26 M. Marya, X. Q. Gayden: Development of requirements for resistance spot welding dual-phase (DP600) steels: Part 1 – The causes of interfacial fracture, Welding Research 11 (2005), pp.172-182
27 V. H. Baltazar Hernandez, M. L. Kuntz, M. I. Khan, Y. Zhou: Influence of microstructure and weld size on the mechanical behaviour of dissimilar AHSS resistance spot welds, Sci. Tech. Weld. Join. 13 (2008), pp. 769-776
DOI:10.1179/136217108X325470
28 F. Hayat, I. Sevim: The effect of welding parameters on fracture toughness of resistance spot-welded galvanized DP600 automotive steel sheets, Int. J. Adv. Manuf. Technol. 58 (2012), pp. 1043-1050
DOI:10.1007/s00170-011-3428-x
29 S. Aslanlar: The effect of nucleus size on mechanical properties in electrical resistance spot welding of sheets used in automotive industry, Mater. Des. 27 (2006), pp. 125-131
DOI:10.1016/j.matdes.2004.09.025
30 B. Kocabekir, R. Kaçar, S. Gündüz, F. Hayat: An effect of heat input, weld atmosphere and weld cooling conditions on the resistance spot weldability of 316L austenitic stainless steel, J. Mater. Process Technol. 195 (2008), pp. 327-335,
DOI:10.1016/j.jmatprotec.2007.05.026
31 M. Vural, A. Akkus, B. Eryurek: Effect of welding nugget diameter on the fatigue strength of the resistance spot welded joints of different steel sheets, J. Mater. Process Technololgy 176 (2006), pp. 127-132
DOI:10.1016/j.jmatprotec.2006.02.026
32 M. I. Khan, M. L. Kuntz, E. Biro, Y. Zhou: Microstructure and mechanical properties of resistance spot welded advanced high strength steels, Mater. Tran. 49 (2008), pp. 1629-1637
DOI:10.2320/matertrans.MRA2008031

Materials Testing downloaded from www.hanser-elibrary.com by Carl Hanser Verlag on November 24, 2015
For personal use only.

Abstract

Neu ermittelte Merkmale des Bruchzähigkeitsverhaltens von punktgeschweißten Dualphasenstahlblechen für Karosserien. Die Bruchzähigkeit ist einer der Parameter, die verwendet werden, um die Lebensdauer von widerstandspunktgeschweißten Verbindungen (Resistance Spot Welds (RSW)) abzuschätzen. Ein punktgeschweißtes Blechpaar wird durch die Scherspannung in der geschweißten Zone beeinflusst, wenn es einer Zugbeanspruchung unterworfen wird. Wiederholte Beanspruchungen reduzieren die Ermüdungslebensdauer der Punktschweißung und der Werkstoff spaltet sich im Bereich der Punktschweißung. In der diesem Beitrag zugrunde liegenden Studie wurde der Effekt der Schweißstromstärke, der Schweißdauer und der Verhältnisse der Keimgrößen auf die Bruchzähigkeit von Widerstandspunktschweißungen von galvanisierten DP 450 Stählen bei verschiedenen Schweißstromstärken und Zeiten untersucht. Die Proben wurden hierzu bei verschiedenen Stromstärken und Zeiten geschweißt. Die Schweißprozesse wurden mit Stromstärken von 3, 5, 7 und 9 kA und 10, 20, 30 und 40 Zyklen (1 Zyklus = 0,02 s) ausgeführt, wobei der Elektrodendruck mit 600 MPa konstant war. Sämtliche Probeserien wurden dem Zugscherversuch unterworfen, um die Bruchzähigkeit zu bestimmen. Die Bruchzähigkeit wurde mit der Gleichung aus der Literatur berechent. Die Linsendurchmesser, die Kerngrößen und die Höhen wurden mittels eines Lichtmikroskops gemessen. Die Mikro-Vickershärte wurde in der Schweißlinse der Wärmeeinflusszone (Heat Affected Zone (HAZ)) und dem Grundwerkstoff analysiert. Die Ergebnisse der Studie zeigen, dass die Bruchzähigkeit der Widerstandspunktschweißungen nicht nur vom Linsendurchmesser D, sondern auch von der Blechdicke t, der Zugkraft F, der Härte H und der Kerngrößenverhältnisse h_n/d_n abhängen.

Bibliography

DOI 10.3139/120.110798
Materials Testing
57 (2015) 11-12, pages 960-967
© Carl Hanser Verlag GmbH & Co. KG
ISSN 0025-5300

The author of this contribution

Dr. Ibrahim Sevim is Associate Professor in the Department of Mechanical Engineering, Engineering Faculty, Mersin University, Turkey. He obtained his PhD degree from the Department of Mechanical Engineering of Istanbul Technical University, Turkey, in 1998. His research areas include failure analysis, welding, modeling and designing applications.